Performance improvement of blue light-emitting diodes with an AlInN/GaN superlattice electron-blocking layer*

Zhao Fang(赵 芳), Yao Guang-Rui(姚光锐), Song Jing-Jing(宋晶晶), Ding Bin-Bin(丁彬彬), Xiong Jian-Yong(熊建勇), Su Chen(苏 晨), Zheng Shu-Wen(郑树文), Zhang Tao(张 涛), and Fan Guang-Han(范广涵)†

Institute of Optoelectronic Materials and Technology, South China Normal University, Guangzhou 510631, *China*
Laboratory of Nanophotonic Functional Materials and Device, South China Normal University, Guangzhou 510631, *China*

(Received 28 August 2012; revised manuscript received 17 December 2012)

The characteristics of a blue light-emitting diode (LED) with an AlInN/GaN superlattice (SL) electron-blocking layer (EBL) are analyzed numerically. The carrier concentrations in the quantum wells, energy band diagrams, electrostatic fields, and internal quantum efficiency are investigated. The results suggest that the LED with an AlInN/GaN SL EBL has better hole injection efficiency, lower electron leakage, and smaller electrostatic fields in the active region than the LED with a conventional rectangular AlGaN EBL or a AlGaN/ GaN SL EBL. The results also indicate that the efficiency droop is markedly improved when an AlInN/GaN SL EBL is used.

Keywords: AlInN/GaN superlattices, efficiency droop, numerical simulation

PACS: 85.60.Jb, 85.50.–n, 87.15.A–, 78.60.Fi **DOI:** 10.1088/1674-1056/22/5/058503

1. Introduction

The efficiency droop is still a big technical challenge for the blue light-emitting diode (LED) to be competitive in high-brightness applications.[1] The internal quantum efficiency (IQE), defined as the fraction of photons generated in the active region to the number of carriers injected into the LED device, usually decreases with a further increasing current. The radiative recombination rate and the output power of the GaN-based LED decrease correspondingly. It is widely known that the electron leakage may play an important role in this issue.[2–4] Recently, some published studies pointed out that the electron confinement by a traditional AlGaN electrn-blocking layer (EBL) is not sufficiently effective to solve the efficiency droop problem.[5,6] Furthermore, the use of the AlGaN EBL can suppress the holes injecting into the active region. Many scientists have tried to use an AlGaN/GaN superlattice (SL) to improve the performance of LEDs.[7–9] It was proposed that the AlGaN/GaN SL in a LED device could prevent the carrier loss over heterostructure barriers.[10,11] However, our research found that the performance improvement by the conventional AlGaN/GaN SL EBL in suppressing the electron overflow and increasing the hole-injection efficiency is limited due to the severe band bending of the EBL caused by a strong static electronic field generated by the lattice mismatch between the GaN and AlGaN interface. Several scientists have tried to relieve the above issues through using special designed EBLs[12–14] or m-plane LED growth.[15] In this paper, we propose to replace the conventional rectangular p-AlGaN and p-AlGaN/p-GaN SL with a p-AlInN/p-GaN superlattice (AlInN/GaN SL) as the EBL. The optical and electrical properties of the blue LED are investigated numerically with APSYS (advance physical model of semiconductor devices) simulation software, which was developed by the Crosslight Software Inc. APSYS software is capable of dealing with the physical properties of LEDs by solving the Poisson equation, current continuity equations, the carrier transport equation, the quantum mechanical wave equation, and the photon rate equation.

2. Structure and parameters

The structure of the original LED used in this paper (denoted as structure A) as a reference was grown on a c-plane sapphire substrate, followed by a 25-nm-thick undoped nucleation GaN layer and a 2.5-μm-thick n-GaN layer (n-doping 5×10^{18} cm^{-3}). The active region was consisted of four 2.2-nm-thick $In_{0.1}Ga_{0.9}N$ quantum wells (QWs) sandwiched by five 15-nm-thick GaN barriers. On the top of the active region were a 20-nm-thick p-$Al_{0.2}Ga_{0.8}N$ EBL (p-doping 5×10^{17} cm^{-3}) and a 0.2-μm-thick p-GaN cap layer (p-doping 7×10^{17} cm^{-3}). The device geometry was designed into a rectangular shape of 300 μm×300 μm. The operating temperature was assumed to be 300 K, and the light extraction efficiency was assumed to be 0.78.[16] Another LED epitaxial structure (denoted as structure B) had a similar layer structure except the conventional rectangular AlGaN EBL was replaced by a 10-pair p-$Al_{0.2}Ga_{0.8}N$/GaN SL EBL (p-doping 5×10^{17} cm^{-3}).

*Project supported by the National Natural Science Foundation of China (Grant No. 61176043) and the Special Funds for Provincial Strategic and Emerging Industries Projects of Guangdong, China (Grant Nos. 2010A081002005, 2011A081301003, and 2012A080304016).

†Corresponding author. E-mail: gfan@scnu.edu.cn

© 2013 Chinese Physical Society and IOP Publishing Ltd

The widths of the $Al_{0.2}Ga_{0.8}N$ SL barriers and wells were both 2 nm. A third structure (denoted as structure C) with special designed SL EBLs was also presented. Its structure was identical to structure B, but the AlGaN/GaN SL was replaced by an $Al_{0.82}In_{0.18}N$/GaN SL as the EBL. These three structures are shown in Fig. 1.

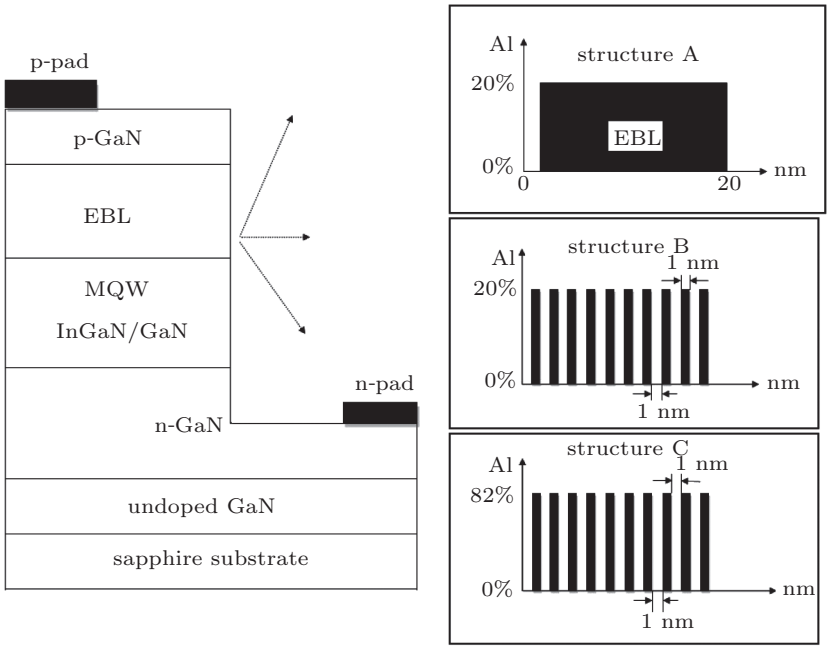


Fig. 1. Schematic diagrams of original LEDs with a conventional rectangular AlGaN EBL (structure A), LEDs with a common ALGaN/GAN SL EBL (structure B), and LEDs with an AlInN/GaN SL EBL (structure C).

The basic equations[17] used to describe the semiconductor device behavior are the Poisson equations

$$-\nabla\cdot\left(\frac{\varepsilon_0\varepsilon_{\rm dc}}{q}\nabla V\right) = -n+p+N_{\rm D}(1-f_{\rm D})-N_{\rm A}f_{\rm A} + \sum_j N_{{\rm t}j}(\delta_j - f_{{\rm t}j}), \quad (1)$$

and the current continuity equations for electrons and holes

$$\nabla\cdot J_{\rm n} - \sum_j R_{\rm n}^{{\rm t}j} - R_{\rm sp} - R_{\rm st} - R_{\rm au} + G_{\rm opt}(t) = \frac{\partial n}{\partial t} + N_{\rm D}\frac{\partial f_{\rm D}}{\partial t}, \quad (2)$$

$$\nabla\cdot J_{\rm p} + \sum_j R_{\rm p}^{{\rm t}j} + R_{\rm sp} + R_{\rm st} + R_{\rm au} - G_{\rm opt}(t) = -\frac{\partial p}{\partial t} + N_{\rm A}\frac{\partial f_{\rm A}}{\partial t}, \quad (3)$$

where $R_{\rm sp}$ is the spontaneous radiative recombination efficiency, $R_{\rm st}$ is the stimulated emission recombination rate, $G_{\rm opt}(t)$ is the optical generation rate, n and p are the carrier concentrations, $N_{\rm D}$ ($N_{\rm A}$) is shallow donor (acceptor) doping concentration, ∇V is the electric field, $N_{{\rm t}j}$ is the density of the j-th SRH deep level traps, δ_1 is the donor, δ_0 is the acceptor, $f_{{\rm t}j}$ is the probability of the j-th deep level traps occupied by electron, $f_{\rm D}$ ($f_{\rm A}$) is the probability of donor (acceptor) occupied by electron (hole), and $\varepsilon_{\rm dc}$ is the relative dielectric constant. These equations govern the electrical behavior (e.g., I–V characteristics) of a semiconductor device.

From the theories of semiconductor device,[17] the carrier flux densities $\boldsymbol{J}_{\rm n}$ and $\boldsymbol{J}_{\rm p}$ in Eqs. (2) and (3) can be written as functions of the carrier concentration and the quasi-Fermi levels

$$\boldsymbol{J}_{\rm n} = n\mu_{\rm n}\nabla E_{\rm fn}, \quad (4)$$

$$\boldsymbol{J}_{\rm p} = p\mu_{\rm p}\nabla E_{\rm fp}, \quad (5)$$

where $E_{\rm fn}$ ($E_{\rm fp}$) is the electron (hole) quasi-Fermi level, $\mu_{\rm n}$ and $\mu_{\rm p}$ are the mobilities of electrons and holes, respectively.

The software treats the carrier recombination due to deep level traps (Shockley–Read–Hall (SRH) recombination) using

$$R_{\rm n}^{{\rm t}j} = c_{{\rm n}j}nN_{{\rm t}j}(1-f_{{\rm t}j}) - c_{{\rm n}j}n_{1j}N_{{\rm t}j}f_{{\rm t}j}, \quad (6)$$

$$R_{\rm p}^{{\rm t}j} = c_{{\rm p}j}pN_{{\rm t}j}f_{{\rm t}j} - c_{{\rm p}j}p_{1j}N_{{\rm t}j}(1-f_{{\rm t}j}), \quad (7)$$

where $c_{{\rm n}j}$ and $c_{{\rm p}j}$ are the capture coefficients for electrons and holes, respectively, $n_{1j}(p_{1j})$ is the carrier concentration when the electron (hole) quasi-Fermi level coincides with energy level $E_{{\rm t}j}$ of the j-th trap.

The Auger recombination rate is given by

$$R_{\rm au} = \left(C_{\rm n}n + C_{\rm p}p\right)\left(np - n_{\rm i}^2\right), \quad (8)$$

where the Auger coefficients $C_{\rm n}$ and $C_{\rm p}$ depend on the type of material simulated, and $n_{\rm i}$ is the intrinsic carrier density.

The band gap energies of InGaN and AlGaN ternary alloys can be expressed as[18]

$$E_{\rm g}(In_xGa_{1-x}N)$$

$$= xE_g(\mathrm{InN}) + (1-x)E_g(\mathrm{GaN}) - 1.4x(1-x),$$

$$E_g(\mathrm{Al}_x\mathrm{Ga}_{1-x}\mathrm{N})$$

$$= xE_g(\mathrm{AlN}) + (1-x)E_g(\mathrm{GaN}) - 0.7x(1-x),$$

$$E_g(\mathrm{Al}_x\mathrm{In}_{1-x}\mathrm{N})$$

$$= xE_g(\mathrm{AlN}) + (1-x)E_g(\mathrm{InN}) - 3.4x(1-x), \quad (9)$$

where E_g(InN), E_g(AlN), and E_g(GaN) are the band gap energies of InN, AlN, and GaN, with the values of 0.78 V, 6.25 V, and 3.4 eV, respectively. Most of the parameters in this paper are the same as those in Ref. [19]. Other material parameters of the devices used in the simulation can be found in Ref. [20]. Zhang *et al*. studied the advantages of blue InGaN LEDs with a special designed AlGaN/GaN SL EBL using these parameters and the same software. A good agreement was obtained between the experimental data and their simulations.

3. Results and discussion

Figure 2 illustrates that the degree of influence on the electrostatic fields in the active region by different EBL is quite different. As can be seen in the figure, the electrostatic fields in the active region of structure A are much stronger than those of the other two structures, especially for the last QW which is near the EBL, and the electrostatic fields in the active region of structure C are the smallest. The stronger electrostatic fields in the active region will lead to a band bending and a poor overlap of electron and hole wave functions, and hence reduce the radiative recombination rate. Thus, structure C has an advantage over the other two structures in radiative recombination due to the smaller electrostatic fields in the active region.

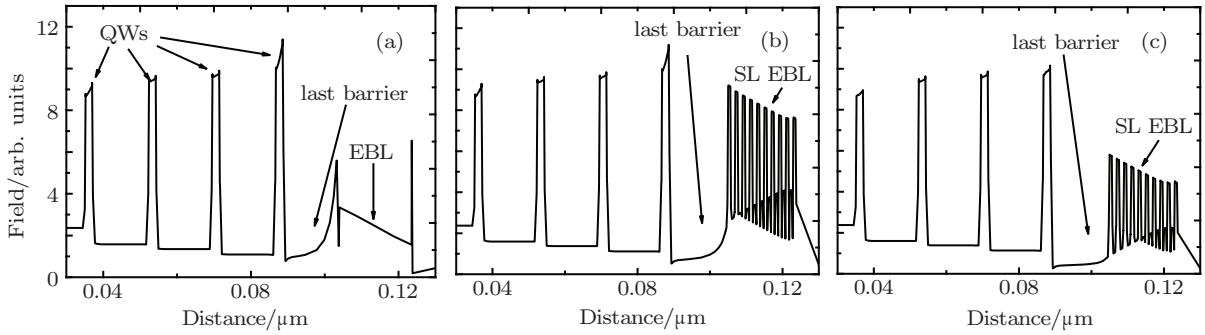


Fig. 2. Electrostatic fields of (a) structure A, (b) structure B, and (c) structure C at 20 mA.

As can be seen in Fig. 3, the piezoelectric polarization field along with the spontaneous polarization field pulls down the energy band at the last GaN QW barrier and the AlGaN EBL interface due to the lattice mismatch. As a result, the effective potential barrier height for electrons in the conduction band of the EBL is reduced and the electron leakage cannot be effectively suppressed. Moreover, because of the band bending effect, the EBL also acts as a potential barrier for holes, which can hinder the injection of holes into the active region. As shown in Fig. 3, the effective potential height for holes in the valance band near the last QW barrier and the AlGaN EBL of structure A (II = 534 meV) is much bigger than that of the other two structures, accordingly, its effective potential height for electrons in the conduction band at the same part (I = 441 meV) is much smaller. As a result, it can be seen in Fig. 3(d) that structure A has the worst electron leakage and the smallest hole injection efficiency. The hole concentration in its active region is much smaller than that of the other two structures. Structure B has smaller band bending around the last barrier and the AlGaN/GaN SL EBL because the SL can reduce the strain forces. However, the lattice mismatch between the last barrier and the SL EBLs is still large enough to generate an effective potential barrier for holes (516 meV). Structure C, with a different AlInN/GaN SL EBL, has the smallest band bending. As can be seen in Fig. 3(c), it has the biggest effective potential barrier for electrons (741 meV) and the smallest effective potential barrier for holes (473 meV). It is apparent in Fig. 3(f) that structure C has the lowest electron leakage and the biggest hole concentrations in the QWs due to the excellent electron blocking effect and the biggest hole injection efficiency.

The corresponding radiative recombination rates in different structures at 20 mA are shown in Fig. 4. For structure A, the radiative recombination rate is dominated by the QW close to the p-type layer as a result of the nonuniform distributions of carriers. While in structures B and C, especially the latter one, due to the enhancement of the carrier concentration and the improvement of the hole carrier transport, the radiative recombination rate is more uniform in QWs and almost all QWs can contribute to the output power. According to the Schrödinger equation, the electron reflectivity of the SL AlInN EBL is much higher than that of the bulk AlInN EBL. In contrast to the AlGaN EBL, the LED with the bulk AlInN EBL showed improved light output power, lower current leakage, and efficiency droop. As a result, more electrons can stay in the active region of the LED with an AlInN SL EBL.[21,22]

SLs can produce a valence-band edge oscillation by employing alloys with different valence-band edge positions. This can increase the overall hole concentration by allowing deep acceptors in the barriers to ionize into the valence band of the neighboring narrow-bandgap material and will partially overcome the low doping efficiency of the deep acceptors. Therefore, as shown in Fig. 4, structure C has the highest total radiative recombination rate and the most uniform recombination rate due to the excellent electron blocking effect and the highest hole-injection efficiency.

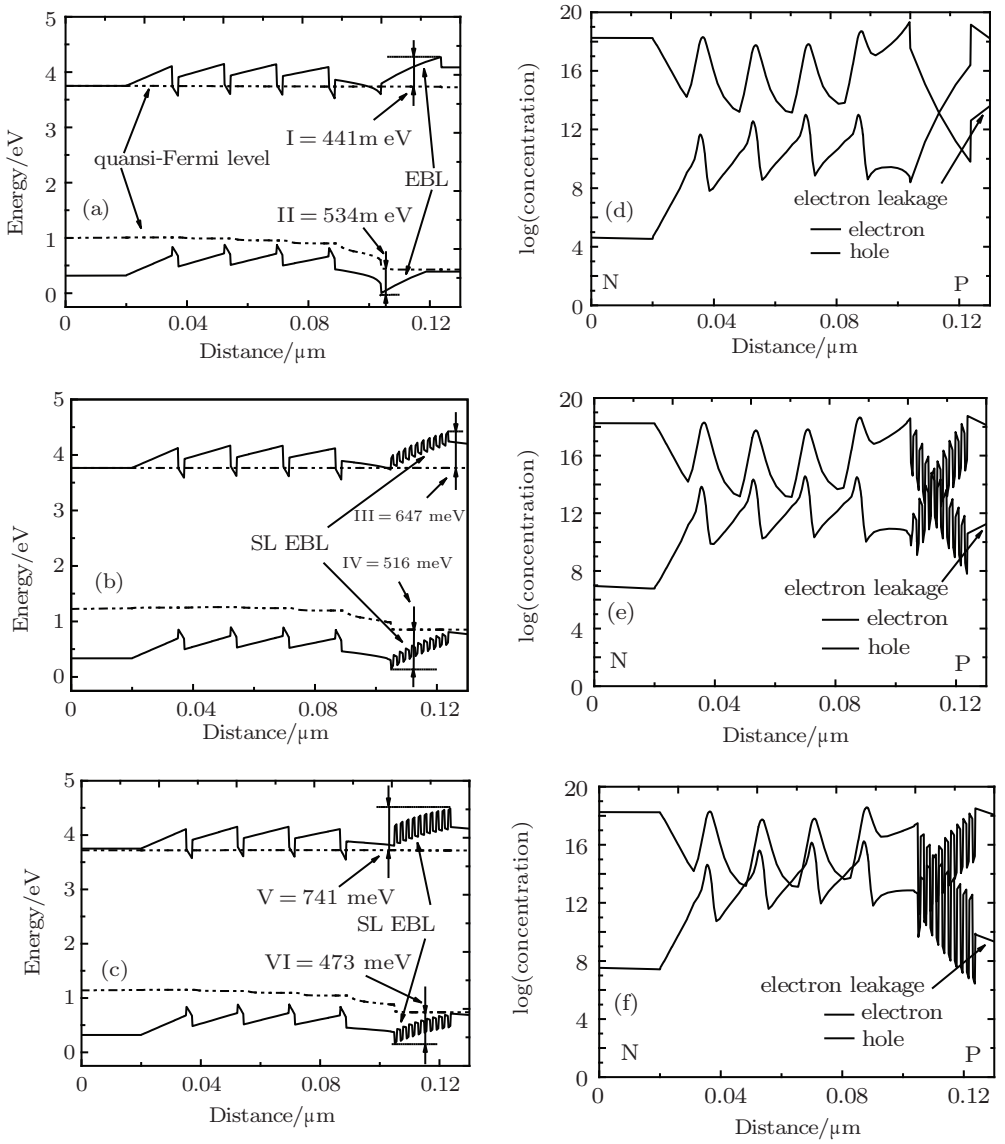


Fig. 3. Energy band diagrams and carrier concentrations of (a), (d) structure A; (b), (e) structure B; and (c), (f) structure C at 20 mA.

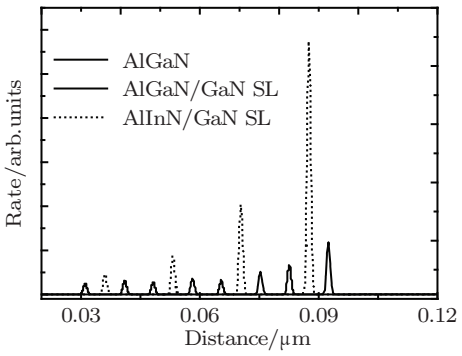


Fig. 4. Radiative recombination rates of LEDs with a conventional rectangular AlGaN EBL, a common AlGaN/GaN SL EBL, and a AlInN/GaN SL EBL.

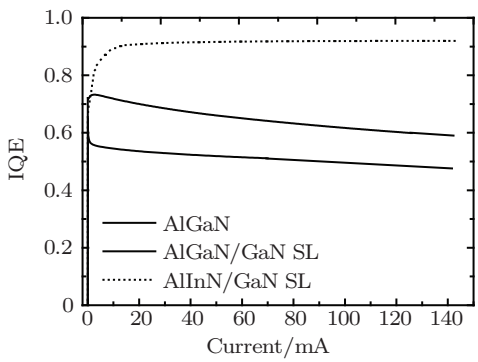


Fig. 5. IQE versus injection current for the three LEDs with different structures.

According to Fig. 5, structure A has the smallest internal quantum efficiency and the worst efficiency droop. Structure C shows the highest IQE and a significantly mitigated efficiency droop. Its better performance is due to the increase of hole injection, the decrease of electron leakage, and the bigger radiative recombination of the QWs.

4. Conclusion

In summary, when the AlInN/GaN SL EBL is used, the hole injection efficiency into the active region from the p-type layer can be greatly increased, the electron leakage can be significantly reduced, and the electrostatic fields in the active region can be considerably relived. The LED with AlInN/GaN SL EBL has a significantly improved optical and electrical performance such as higher IQE and much bigger recombination. Furthermore, the efficiency droop of this structure is markedly improved.

References

[1] Yang L, Ma X H, Feng Q and Hao Y 2008 *Chin. Phys. B* **17** 2696

[2] Lu Y, Yang Z J, Pan Y B, X K, Hu X D, Zhang B and Zhang G Y 2006 *Chin. Phys. Lett.* **23** 256

[3] Chen J, Fan G H and Zhang Y Y 2012 *Acta Phys. Sin.* **61** 178504 (in Chinese)

[4] Zhang Y Y and Fan G H 2011 *Acta Phys. Sin.* **60** 078504 (in Chinese)

[5] Xie J Q, Ni X F, Fan Q, Shimada R, Özgür Ü and Morkoc H 2008 *Appl. Phys. Lett.* **93** 121107

[6] Rozhansky I V and Zakheim D A 2007 *Phys. Status Solidi A* **204** 227

[7] Kumakura K and Kobayashi N 1999 *Jpn. J. Appl. Phys.* **38** L1012

[8] Kozodoy P, Hansen M, DenBaars P S and Mishra K U 1999 *Appl. Phys. Lett.* **74** 3681

[9] Dingle R, Störmer L H, Gossard C A and Wiegmann W 1978 *Appl. Phys. Lett.* **33** 665

[10] Wang C L, Tsai M C, Gong J R, Liao W T, Lin P Y, Yen K Y, Chang C C, Lin H Y and Hwang S K 2007 *Mater. Sci. Eng. B* **138** 180

[11] Gong C C, Fan G H, Zhang Y Y, Xu Y Q, Liu X P, Zheng S W, Yao G R and Zhou D T 2012 *Chin. Phys. B* **21** 068505

[12] Wang C H, Ke C C, Lee C Y, Chang S P, Chang W T, Li J C, Li Z Y, Yang H C, Kuo H C, Lu T C and Wang S C 2010 *Appl. Phys. Lett.* **97** 261103

[13] Kuo Y K, Chang J Y and Tsai M C 2010 *Opt. Lett.* **35** 3285

[14] Choi S, Kim H J, Kim S S, Liu J, Kim J, Ryou J H, Dupuis R D, Fischer A M and Ponce F A 2010 *Appl. Phys. Lett.* **96** 221105

[15] Ling S C, Lu T C, Chang S P, Chen J R, Kuo H C and Wang S C 2010 *Appl. Phys. Lett.* **96** 231101

[16] Wang T H, Chang J Y, Tsai M C and Kuo Y K 2011 *Proc. SPIE* **7954** 79541

[17] Zse M S 1981 *Physics of Semiconductor Devices* (2nd edn.) (New York: John Wiley & Sons)

[18] Stringfellow G B and Craford M G 1997 *High Brightness Light Emitting Diodes* (San Diego: CA Academic) p. 412

[19] Kuo Y K, Chang J Y, Tsai M C and Yen S H 2009 *Appl. Phys. Lett.* **95** 011116

[20] Vurgaftman I and Meyer J R 2003 *J. Appl. Phys.* **94** 3675

[21] Lee N S, Cho S Y, Ryu H Y, Son J K, Paek H S, Sakong T, Jang T, Choi K K, Ha K H, Yang M H, Nam O H and Park Y 2006 *Appl. Phys. Lett.* **88** 111101

[22] Lu T P, Li S T, Zhang K, Liu C, Xiao G W, Zhou Y G, Zheng S W, Yin Y A, Wu L J, Wang H L and Yang X D 2011 *Chin. Phys. B* **20** 098503